FINAL VERSION ACCEPTED

Synthesis of Chiral Iron-Based Ionic Liquids: Modelling Stable Hybrid Materials†

Carmen Martin,[a,b,*] Israel Cano,[c,*] Fabio Scé,[a] Rubén Pérez-Aguirre,[d] Carolina Gimbert-Suriñach,[e] Pilar Lopez-Cornejo[b] and Imanol de Pedro[a]

ABSTRACT: Five chiral iron-containing ionic liquids were synthetized from several chiral ionic liquids (CILs) based on different imidazolium cations. These novel compounds were prepared through an easy synthetic method consisting in mixing 1 equivalent of iron salt FeX_3 (X = Cl or Br) and 1 equivalent of chiral ionic liquid. The so-obtained chiral iron-based ionic liquids contain easily tunable imidazolium cations, which allow the preparation of a wide range of compounds within different functional groups and chiral moieties. These chiral iron-based ionic liquids have been fully characterized by a wide variety of techniques, including polarimetry, inductively coupled plasma optical emission spectrometry, elemental analysis, thermogravimetric analysis, differential scanning calorimetry, magnetic susceptibility measurements, and UV-vis, attenuated total reflection Fourier-transform infrared and Raman spectroscopies. Such experiments confirmed the structure of these newly materials, as well as their appealing properties. The combination of a chiral moiety with a haloferrate anion within the ILs structure allows the formation of very stable and multifunctional compounds with promising chiral, magnetic, optical and acidic properties. The resulting chiral iron-based ILs exhibit great potential for use in a range of applications such as enantioselective catalysis or chiral recognition, to name a few.

Keywords: Acidic chiral paramagnetic ionic liquid • hybrid material • imidazolium-based halometallate complex • iron-containing ionic liquid

[a] *Universidad de Cantabria, CITIMAC, Facultad de Ciencias, Avda. de los Castros s/n, 39005 Santander, Spain.*
[b] *Universidad de Sevilla, Department of Physical Chemistry, Faculty of Chemistry, c/Profesor García González s/n, 41012 Sevilla, Spain.*
[c] *School of Chemistry, University of Nottingham, NG7 2RD, Nottingham, UK.*
[d] *Universidad del País Vasco, Departamento de Química Inorgánica, Facultad de Ciencia y Tecnología, Apartado 644, E-48080, Bilbao, Spain.*
[e] *Institute of Chemical Research of Catalonia (ICIQ). Avinguda Països Catalans 16, 43007 Tarragona, Spain.*
† Electronic supplementary information (ESI) available: Crystallographic data, analytical and spectral data. CCDC: 1961691 and 1962239.

INTRODUCTION

Multifunctional compounds based on ionic liquids (ILs) have gained considerable interest owing to the unique properties of ILs (e.g., good thermal stability, high ionic conductivity and wide electrochemical stability window).[1,2,3,4] In particular, acidic ionic liquids (AILs) have been extensively investigated due to their capability to act as membranes, electrolytes for batteries and capacitors or catalysts (e.g., depolymerisation of cellulose, production of biodiesel, oxidation reactions, etc.).[5,6] Among them, halometallate-based ILs[7] are an important subgroup of AILs which contain a metal-based Lewis acid within their structure. This metal component enhances their features against purely organic ILs, such as lower viscosities and higher conductivities, and makes them very interesting compounds for a number of applications, including electrical-energy storage[8] and catalysis (e.g. Friedel–Crafts reactions, Michael addition and polyethylene terephthalate (PET) glycolysis).[9,10,11,12] Interestingly, their architecture can be easily modulated to create tailor-made ILs with different physical and chemical properties. In this regard, chiral centers or magnetic moieties within ILs structures can improve the AILs performance (e.g. in catalysis) and tune their properties. However, the development of new materials with simultaneous chiral, magnetic and acidic characteristic is still in its infancy and only two articles have been reported on the preparation of acidic chiral paramagnetic ionic liquids (ACMILs).[13,14] Among them, it is worth mentioning the work of Warner and co-workers, in which the synthesis of chloroferrate(III) chiral ILs incorporating amino acid derived cations and their use as chiral recognition agents of fluorescent analytes is described.[13]

Recently, our group has developed new halometallate ILs based on iron.[15,16,17] We have shown that these so-called halometallate-based ILs (containing a Lewis acid and a nucleophile within the structure) display a good catalytic activity in the glycolysis of PET, leading to better yields and selectivities than those reported with purely organic ILs.[16,17] In a next step, we have decided to extend this work introducing chiral features into the AILs structures. In this context, the imidazolium cation is easily tunable and allows the introduction of functional groups and chiral moieties, opening the door to an enormous variety of compounds. Thus, herein we report the synthesis of five new and stable chiral imidazolium-based haloferrate(III) ILs with diverse architectures (Fig. 1). To investigate their stability and appealing chiral/magnetic properties, a detailed characterization of these multifunctional ILs was performed by the state-of-the-art techniques, such as polarimetry, inductively coupled plasma optical emission spectrometry (ICP-OES), elemental analysis (EA), thermogravimetric analysis (TGA), differential scanning calorimetry (DSC), UV-vis spectroscopy, magnetic susceptibility measurements, and

attenuated total reflection Fourier-transform infrared (ATR FT-IR) and Raman spectroscopies. These switchable ACMILs may be promising candidates as enantioselective catalysts (e.g. CO_2 fixation into cyclic carbonates)[18] or chiral recognition agents.[13]

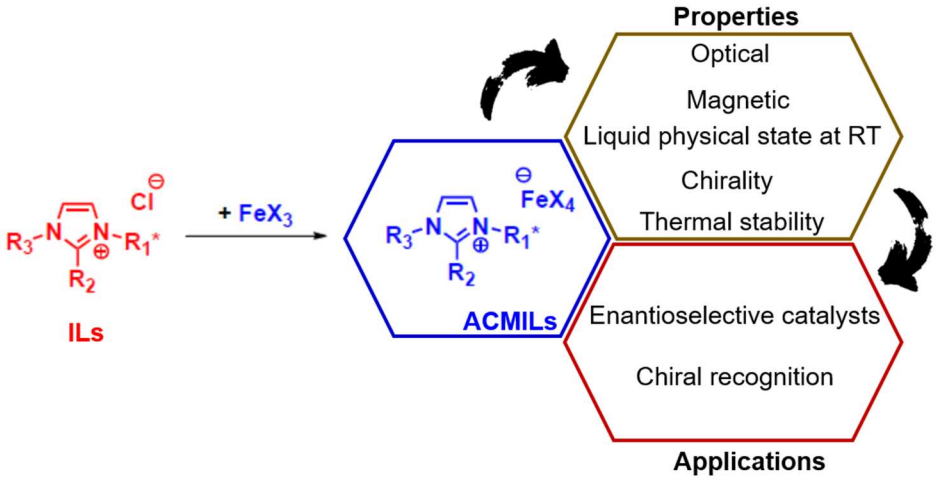

Fig. 1 Overall scheme of the preparation of ACMLs, properties and applications.

Therefore, the main objective of this work is the preparation of a series of new multifunctional ILs by the precise design of the imidazolium cation structure and the appropriate selection of the anion.

EXPERIMENTAL

General Procedures

Solvents were purchased from Sigma-Aldrich as HPLC grade and dried by means of an Inert Puresolv MD purification system. All reagents were purchased from commercial suppliers (Sigma Aldrich and Across) and purified when required by literature procedures.[19] The ion exchange resin Amberlite IRA-402(OH) was supplied by Alfa Aesar.

Elemental analysis (EA). Elemental analyses were performed by the Elemental Analysis Service of the University of Nottingham.

Nuclear magnetic resonance (NMR). ^{1}H and ^{13}C NMR spectra were recorded on a Bruker AV3400 400 MHz and a Bruker DPX500 500 MHz nuclear magnetic resonance spectrometers, and referenced to the residual NMR solvent signals. Signals are quoted as s (singlet), d (doublet), t (triplet), dd (double doublet), td (triplet doublet) and m (multiplet).

Electrospray ionization mass spectrometry (ESI-MS). ESI-MS analyses were carried out on a Bruker ESI-TOF MicroTOF II and Orbitrap Elite (Thermo Scientific) spectrometers.

Fourier transform infrared spectroscopy (FT-IR). FT-IR measurements were performed on a Bruker Alpha Series FT-IR spectrometer equipped with an attenuated total reflectance (ATR) module. The ATR FT-IR spectra were recorded by collecting 24 scans of a compound in the ATR module.

Non-polarized Raman spectra. The non-polarized Raman spectra were recorded in the backscattering geometry with a Horiba T64000 triple spectrometer with a confocal microscope in the subtractive mode which had a resolution of 0.6 cm^{-1}, a 1800 grooves/mm grating and a 100-μm slit was equipped with a liquid N_2-cooled CCD detector (Jobin-Yvon Symphony). A 647 nm line of a Coherent Innova Spectrum 70C Ar^+-Kr^+ laser was focused down with a 20x objective and kept the power on the sample below 5 mW to avoid laser-heating effects on the material being tested and the concomitant softening of the observed Raman peaks.

UV-vis spectroscopy. UV−vis measurements were carried out on a Shimadzu UV-2401PC spectrophotometer equipped with a photomultiplier detector, double beam optics, and D2 and W light sources. Samples were measured at 25°C and with dimethylformamide (DMF) as solvent.

Differential scanning calorimetry (DSC). DSC measurements were carried out on a TA instruments Discovery from -90 °C to 150 °C at a rate of 10 °C/min under nitrogen atmosphere.

Thermogravimetric analysis (TGA). Thermogravimetric measurements were carried out on a TA instruments Discovery at a heating rate of 10 °C/min and in a temperature range from 100 °C to 1000 °C under N_2 in a platinum crucible. Note that the decomposition temperature (T_d) was determined by TGA at 10% weight loss of the analyte.

Inductively coupled plasma optical emission spectrometry (ICP-OES). The iron content determination was performed through analysis of the samples by ICP-OES on a Perkin Elmer Optima 2000 DV ICP-OES. The samples were prepared by diluting 25 mL of ionic liquid with approximated iron concentration of 150 mg/L (ppm) in HNO_3 with a concentration of 2% (v/V). Calibration curves were prepared using standard solutions of concentrations between 0–250 ppm prepared by dilution of the standard solution. The iron Standard for ICP TraceCERT® (10′000 mg/L Fe in nitric acid) was supplied by Sigma Aldrich.

Magnetization measurements. DC magnetic susceptibility measurements for ionic liquids **5-9** were carried out in a Quantum Design MPMS SQUID magnetometer using a

field of 1 kOe in the 2-300 K temperature range. Magnetization as a function of field (H) was measured using the same magnetometer in the -50 ≤ H/kOe ≤ 50 at 2 K after cooling the sample in zero field.

Polarimetry. Optical rotations were measured in a 1.0 dm tube with a Perkin Elmer spectropolarimeter (model 341) equipped with a Na lamp.

X-ray crystal structure determinations (CCDC: 1961691 for **1** and 1962239 for **4**). X-ray crystal structure determinations were performed at the X-ray Service of the University of Nottingham. Crystals suitable for X-ray diffraction were selected and covered with "fomblin" (YR-1800 perfluoropolyether oil). The crystal was then mounted on a polymer-tipped MicroMount™ and cooled to 120 K. Single crystal X-ray diffraction data were collected using an Agilent SuperNova diffractometer, Atlas CCD area detector (mirror-monochromated Cu-*Kα* radiation source; *λ* = 1.54184 Å or graphite-monochromated Mo-Kα radiation source; *λ* = 0.7103 Å; ω scans) and an Agilent SuperNovaII diffractometer Titan S2 CCD area detector (mirror monochromated Cu-*Kα* radiation source; *λ* = 1.54184 Å; *ω* scans). Crystal structures were solved and refined by means of the Olex2 software package,[20,21] program using Charge Flipping and refined with the ShelXL.[22] Crystallographic data have been deposited in the Cambridge Crystallographic Data Center under reference numbers CCDC 1961691 and 1962239 for CILs **1** and **4**, respectively. These data can be obtained free of charge *via* www.ccdc.cam.ac.uk/data_ request/cif.

Gas Chromatography (GC). Analyses (determination of enantiomeric excess) of the reaction mixtures were performed on a Thermo Scientific Trace 1310 Gas Chromatograph with a Lipodex A (hexakis-(2,3,6-tri-O-pentyl)-α-cyclodextrin) 25m column.

Synthetic Procedures

Synthesis of chiral imidazolium-based ionic liquids.

- *(S)-1-(2-Methylbutyl)-2,3-dimethylimidazolium chloride ([S-methylBMMIm]Cl, **1**).* (*S*)-(+)-1-Chloro-2-methylbutane (12.0 g, 0.11 mol, 1.10 equivalents) and 1,2-dimethyl-1*H*-imidazole (9.81 g, 0.10 mol, 1.00 equivalent) were dissolved in 5.50 mL of CH_3CN in a round bottom flask under inert atmosphere. The reaction mixture was heated for 5 days at 100 °C under reflux. Afterwards, the solution was cooled to room temperature (R.T.) and the volatile materials were evaporated under vacuum. The remaining orange oil was re-dissolved in the minimum amount of dry CH_3CN and added dropwise *via* cannula to a well-stirred solution of ethyl acetate (CH_3CN:ethyl acetate ratio *ca.* 1:5). Once the addition of the CH_3CN solution was completed, the mixture was cooled at -30 °C in the freezer to crystallize. The final product was washed with ethyl acetate and dried under

vacuum, obtaining a pale yellow powder. Yield: 12.1 g (0.06 mol, 65 %). Crystals of **1** suitable for X-ray diffraction analysis were obtained at R.T. by slow diffusion of ethyl acetate vapour into an CH_3CN solution of **1**. ^{1}H NMR (400 MHz, $CDCl_3$): δ = 7.88 (d, $^3J_{HH}$ = 2.0 Hz, 1H, CH_{Ar}), 7.44 (d, $^3J_{HH}$ = 2.0 Hz, 1H, CH_{Ar}), 4.08 (dd, $^2J_{HH}$ = 15.0 Hz and $^3J_{HH}$ = 7.5 Hz, 1H, NCH_2), 4.08 (s, 3H, NCH_3), 3.94 (dd, $^2J_{HH}$ = 14.0 Hz and $^3J_{HH}$ = 9.0 Hz, 1H, NCH_2), 2.77 (s, 3H, NCCH_3), 1.90-1.77 (m, 1H,CHCH$_3$), 1.44-1.32 (m, 1H, CH_2CH$_3$), 1.26-1.14 (m, 1H, CH_2CH$_3$), 0.90 (t, $^3J_{HH}$ = 7.0 Hz, 3H, CH$_2$CH_3), 0.89 (d, $^3J_{HH}$ = 6.0 Hz, 3H, CHCH_3). ^{13}C NMR (101 MHz, $CDCl_3$): δ = 143.8 (1C, N*C*N), 123.4 (1C, *C*H$_{Ar}$), 121.7 (1C, *C*H$_{Ar}$), 54.6 (1C, N*C*H$_2$), 36.1 (1C, N*C*H$_3$), 35.7 (1C, NC*C*H$_3$), 26.6 (1C, *C*HCH$_3$), 16.62 (1C, *C*H$_2$CH$_3$), 11.1 (1C, CH*C*H$_3$), 10.8 (1C, CH$_2$*C*H$_3$). ESI-MS (+ ve): m/z = 167.1553 $[M\text{-}Cl]^+$ (calculated: m/z = 167.1548). Characteristic IR bands (cm^{-1}): 3121-3022 (C-H sp^2), 2960-2849 (C-H sp^3), 1587 (C=C/C=N), 1536 (C-C/C-N), 1120(C-N), 910 (C-H sp^2), 820 (C-H sp^2), 758 (C-H sp^2). $[\alpha]_D^{25} = -2.4$ (c = 5 mg/1 mL MeOH). T_d = 250 ºC. (Fig. S1, S2, S7, S18, S26 and S51 in Supporting Information).

- *(R)-3-(2,3-Dihydroxypropyl)-1-methylimidazolium chloride ([R-diOHPrMIm]Cl, **2**) and (S)-3-(2,3-dihydroxypropyl)-1-methylimidazolium chloride ([S-diOHPrMIm]Cl, **3**)*. **2** and **3** were prepared according to procedures described in the literature.[23] the (*R*) or (*S*)-3-Chloro-1,2-propanediol (12.2 g, 0.11 mol, 1.10 equivalents) was placed in a round bottom flask with a stirring bar and dissolved in CH_3CN (10.0 mL) under inert atmosphere. After addition of 1-methyl-1*H*-imidazole (9.55 g, 0.10 mol, 1.0 equivalent), the reaction mixture was heated at 90 °C for 48 h under reflux. Upon completion of the reaction, the solvent was removed *in vacuo*. Then, the reaction crude was re-dissolved in the minimum amount of dry CH_3CN and added dropwise *via* cannula to a well-stirred solution of ethyl acetate (CH_3CN:ethyl acetate ratio *ca.* 1:5). Finally, the mixture was cooled at -30 °C in the freezer to crystallize. The final product was washed with ethyl acetate and dried under vacuum, obtaining a pale orange powder. Yield: 15.4 g (0.08 mol, 80 %). ^{1}H NMR (400 MHz, D_2O): δ = 8.77 (s, 1H, N-C*H*-N), 7.52 (m, 1H, CH_{Ar}), 7.48 (m, 1H, CH_{Ar}), 4.40 (dd, $^2J_{HH}$ = 15.0 Hz and $^3J_{HH}$ = 3.0 Hz, 1H, NCH_2), 4.22 (dd, $^2J_{HH}$ = 14.5 Hz and $^3J_{HH}$ = 3.5 Hz, 1H, NCH_2), 4.11-4.04 (m, 1H, C*H*OH), 3.93 (s, 3H, NCH_3), 3.63 (dd, $^3J_{HH}$ = 5.0 Hz and $^3J_{HH}$ = 1.5 Hz, 2H, CH_2OH). ^{13}C NMR (101 MHz, D_2O): δ = 136.6 (1C, N*C*HN), 123.5 (1C, *C*H$_{Ar}$), 122.9 (1C, *C*H$_{Ar}$), 69.8 (1C, *C*HOH), 62.4 (1C, *C*H$_2$OH), 51.7 (1C, N*C*H$_2$), 35.7 (1C, N*C*H$_3$). ESI-MS (+ ve): m/z = 157.0979 $[M\text{-}Cl]^+$ (calculated: m/z = 157.0977). Characteristic IR bands (cm^{-1}): 3325 (O-H), 3210 (O-H), 3165-3058 (C-H sp^2), 2933-2830 (C-H sp^3), 1632 (C=C/C=N), 1558 (C-C/C-N), 1164 (C-N), 1109 (C-O), 1059 (C-O), 941 (C-H sp^2), 846 (C-H sp^2), 773 (C-H sp^2). (Fig. S3, S4, S8 and S19).

R-[diOHPrMIm]Cl, **2:** $[\alpha]_D^{25} = +15.6$ (c = 5 mg/1 mL MeOH). T_d (10%) = 300 ºC. (Fig. S27).

S-[diOHPrMIm]Cl, **3**: $[\alpha]_D^{25} = -16.0$ (c = 5 mg/1 mL MeOH). T_d (10%) = 280 ºC. (Fig. S28).

- *1-((1S,2R,4S)-(+)-Menthoxymethyl)-2,3-dimethylimidazolium chloride ([R-menthyl MMIm]Cl, **4**)*. **4** was prepared according to procedures described in the literature.[24] (1*S*,2*R*,4*S*)-(+)-Chloromethyl menthyl ether (5.00 g, 24.4 mmol, 1.05 equivalents) and 1,2-dimethyl-1*H*-imidazole (1.00 g, 23.2 mmol, 1.00 equivalents) were dissolved in CH_3CN (75 mL) in a round bottom flask under inert atmosphere. The reaction mixture was heated for 24 h at 90 °C under reflux. Next, the solution was cooled to R.T. and the solvent was evaporated under vacuum. Finally, the product was washed three times with diethyl ether and dried under vacuum to give a white powder. Yield = 6.27 g (20.9 mmol, 90 %). Crystals of **4** suitable for X-ray diffraction analysis were obtained at 6 ºC in CH_3CN. ^{1}H NMR (400 MHz, $CDCl_3$): δ = 7.88 (d, $^3J_{HH}$ = 2.0 Hz, 1H, CH_{Ar}), 7.77 (d, $^3J_{HH}$ = 2.0 Hz, 1H, CH_{Ar}), 5.71 (d, $^2J_{HH}$ = 11.0 Hz, 1H, NCH_2O), 5.64 (d, $^2J_{HH}$ = 11.0 Hz, 1H, NCH_2O), 4.02 (s, 3H, NCH_3), 3.30 (td, $^3J_{HH}$ = 10.0 Hz and $^3J_{HH}$ = 4.0 Hz, 1H, OC*H*), 2.83 (s, 3H, NCCH_3), 2.09-2.03 (m, 1H, CH_2), 1.97-1.87 (m, 1H, CH_2), 1.97-1.87 (m, 1H, CHC*H*(CH_3), 1.69-1.58 (m, 2H, CH_2), 1.45-1.32 (m, 1H,C*H*CH_3), 1.26-1.18 (m, 1H, C*H*CH(CH_3)$_2$), 0.95-0.88 (m, 2H, CH_2), 0.92 (d, $^3J_{HH}$ = 6.6 Hz, 3H, CHCH_3), 0.88 (d, $^3J_{HH}$ = 7.5 Hz, 3H, CHCH(CH_3)$_2$), 0.51 (d, $^3J_{HH}$ = 7.0 Hz, 3H, CHCH(CH_3)$_2$). ^{13}C NMR (101 MHz, $CDCl_3$): δ = 145.1 (1C, N*C*N), 123.0 (1C, *C*H$_{Ar}$), 121.8 (1C, C$_{Ar}$), 79.6 (1C, OCH), 76.4 (1C, NCH_2O), 47.9 (1C, CH_2), 40.4 (1C, *C*H_2),35.9 (1C, N*C*H_3), 34.2 (1C, *C*HCH(CH_3)$_2$), 31.4 (1C, *C*HCH_3), 25.6 (1C, CH*C*H(CH_3)$_2$), 22.9 (1C,*C*H_2), 22.3 (1C, CH*C*H_3), 21.0 (1C, CHCH(*C*H_3)$_2$), 15.7 (1C, CHCH(*C*H_3)$_2$), 10.8 (1C, NC*C*H_3). ESI-MS (+ ve): m/z = 265.2276 $[M\text{-}Cl]^+$ (calculated: m/z = 265.2280). Characteristic IR bands (cm^{-1}): 3159-3072 (C-H sp^2), 2960-2855 (C-H sp^3), 1634 (C=C/C=N), 1571 (C-C/C-N), 1166 (C-O-C), 1042 (C-O-C), 838 (C-H sp^2), 747 (C-H sp^2). $[\alpha]_D^{25} = +112.0$ (c = 5 mg/1 mL MeOH). T_d = 212 ºC. (Fig. S5, S6, S9, S20, S29 and S52). ^{1}H and ^{13}C NMR, ESI-MS, FT-IR and $[\alpha]_D^{20}$ data were consistent with those previously reported.[24]

Synthesis of iron-containing ionic liquids. 1.0 equivalent of $FeCl_3$ was mixed with 1.0 equivalent of the corresponding imidazolium salt (**1**–**4**) in a Schlenk flask under Ar atmosphere (glovebox). After stirring for 12 h at 90 ºC, the acidic chiral paramagnetic ionic liquids **5–7** and **9** were obtained with quantitative conversion. Similarly, the acidic chiral paramagnetic ionic liquid **8** was prepared by mixing 1.0 equivalent of $FeBr_3$ with 1.0 equivalent of (*S*)-3-(2,3-dihydroxypropyl)-1-methylimidazolium bromide (*S*-[diOHPrMIm]Br). The reaction was stirred under Ar atmosphere for 12 h at 90 ºC to obtain **8**.

S-[diOHPrMIm]Br synthesis*:* A solution containing 950.0 mg of **3** (4.9 mmol) in 5 mL of H_2O was passed through a column packed with anion-exchange Amberlite resin IRA-402(OH) using H_2O as eluent. Afterwards,4.9 mmol of HBr (aq.) 48 wt% was added to the aqueous solution of the hydroxide form of **3** collected. After addition of HBr, the reaction mixture was stirred overnight at R.T. Upon completion of the reaction the solvent was removed *in vacuo* (rotary evaporator), yielding *S-[diOHPrMIm]Br*.

*- (S)-1-(2-Methylbutyl)-2,3-dimethylimidazolium tetrachloroferrate(III) ([S-methylBMMIm][FeCl₄], **5**).* ESI-MS (+ ve): m/z = 167.15 $[M\text{-}FeCl_4]^+$ (calculated: m/z = 167.1548). ESI-MS (- ve): m/z = 197.81 $[FeCl_4]^-$ (calculated: m/z = 197.8074). Elemental Analysis: Obs. C, 32.07; H, 5.11; N, 7.82. Calc. C, 32.91; H, 5.25; N, 7.68. ICP-OES (% weight): Obs. Fe, 14.81. Calc. Fe, 15.30. Characteristic IR bands (cm^{-1}): 3178-3086 (C-H sp^2), 2966-2854 (C-H sp^3), 1586 (C=C/C=N), 1536 (C-C/C-N), 1165 (C-N), 837 (C-H sp^2), 804 (C-H sp^2), 739 (C-H sp^2). Raman (cm^{-1}): 334, 332, 141, 110 (Fe-Cl). $[\alpha]_D^{25} = -2.6$ (c = 5 mg/1 mL MeOH). T_d (10%) = 334 ºC and T_g = -63 ºC. UV-Vis [λmax/nm (ε/$M^{-1}\cdot cm^{-1}$)]: 315 (20000), 364 (18666). μ_{eff} = 5.88 μ_B/molecule. (Fig. S10, S11, S21, S30, S31, S40 and S45).

*- (R)-3-(2,3-Dihydroxypropyl)-1-methylimidazolium tetrachloroferrate(III) ([R-diOHPr MIm][FeCl₄], **6**)*. ESI-MS (+ ve): m/z = 157.0970 $[M\text{-}FeCl_4]^+$ (calculated: m/z = 157.0972). ESI-MS (- ve): m/z = 197.8073 $[FeCl_4]^-$ (calculated: m/z = 197.8074). Elemental Analysis: Obs. C, 22.35; H, 3.72; N, 7.04. Calc. C, 23.69; H, 3.69; N, 7.89. ICP-OES (% weight): Obs. Fe, 14.75. Calc. Fe, 15.74. Characteristic IR bands (cm^{-1}): 3513 (O-H), 3364 (O-H), 3149-3096 (C-H sp^2), 2962-2881 (C-H sp^3), 1690 (C=C/C=N), 1556 (C-C/C-N), 1164 (C-N), 1096 (C-O), 1037 (C-O), 926 (C-H sp^2), 829 (C-H sp^2), 740 (C-H sp^2). Raman (cm^{-1}): 330, 328, 138, 108 (Fe-Cl). $[\alpha]_D^{25} = +12.2$ (c = 5 mg/1 mL MeOH). T_d (10%) = 259 ºC and T_g = -35 ºC. UV-Vis [λmax/nm (ε/$M^{-1}\cdot cm^{-1}$)]: 316 (84000), 364 (85000). μ_{eff} = 5.89 μ_B/molecule. (Fig. S12, S13, S22, S32, S33, S41 and S46).

*- (S)-3-(2,3-Dihydroxypropyl)-1-methylimidazolium tetrachloroferrate(III) ([S-diOHPr MIm][FeCl₄], **7**).* ESI-MS (+ ve): m/z =157.0970 $[M\text{-}FeCl_4]^+$ (calculated: m/z = 157.0972). ESI-MS (- ve): m/z = 197.8073 $[FeCl_4]^-$ (calculated: m/z = 197.8074). Elemental Analysis: Obs. C, 22.54; H, 3.70; N, 7.02. Calc. C, 23.69; H, 3.69; N, 7.89. ICP-OES (% weight): Obs. Fe, 15.24. Calc. Fe, 15.74. Characteristic IR bands (cm^{-1}): 3513 (O-H), 3364 (O-H), 3149-3096 (C-H sp^2), 2962-2881 (C-H sp^3), 1690 (C=C/C=N), 1556 (C-C/C-N), 1164 (C-N), 1096 (C-O), 1037 (C-O), 926 (C-H sp^2), 829 (C-H sp^2), 740 (C-H sp^2). Raman (cm^{-1}): 332, 330, 140, 111 (Fe-Cl). $[\alpha]_D^{25} = -13.6$ (c = 5 mg/1 mL MeOH). T_d (10%) = 257 ºC and T_g = -34 ºC. UV-Vis [λmax/nm (ε/$M^{-1}\cdot cm^{-1}$)]: 317 (12750), 363 (10500). μ_{eff} = 5.88 μ_B/molecule. (Fig. S23, S34, S35, S42 and S47).

- *(S)-3-(2,3-Dihydroxypropyl)-1-methylimidazolium tetrabromoferrate(III) ([S-diOHPr MIm][FeBr$_4$], **8**).* ESI-MS (+ ve): m/z = 157.0970 $[M\text{-}FeBr_4]^+$ (calculated: m/z = 157.0972). ESI-MS (- ve): m/z = 375.6045 $[FeBr_4]^-$ (calculated: m/z = 375.6042). Elemental Analysis: Obs. C, 14.76; H, 2.19; N, 5.03. Calc. C, 15.74; H, 2.46; N, 5.26. ICP-OES (% weight): Obs. Fe, 10.83. Calc. Fe, 10.48. Characteristic IR bands (cm^{-1}): 3529 (O-H), 3370 (O-H), 3155-3099 (C-H sp^2), 2961-2875 (C-H sp^3), 1690 (C=C/C=N), 1563 (C-C/C-N), 1168 (C-N), 1099 (C-O), 1039 (C-O), 925 (C-H sp^2), 825 (C-H sp^2), 741 (C-H sp^2). Raman (cm^{-1}): 295, 198 (Fe-Br). $[\alpha]_D^{25} =$ -18.4 (c = 5 mg/1 mL MeOH). T_d (10%) = 275 ºC and T_g = -31 ºC. UV-Vis [λmax/nm (ε/$M^{-1}\cdot cm^{-1}$)]: 394(3333), 426 (2619), 473, (3048). μ_{eff} = 6.09 μ_B/molecule. (Fig. S14, S15, S24, S36, S37, S43 and S48).

- *(R)-1-((1S,2R,4S)-(+)-Menthoxymethyl)-2,3-dimethylimidazolium tetrachloro ferrate(III) ([R-menthylMMIm][FeCl$_4$], **9**).* ESI-MS (+ ve): m/z = 265.2280 $[M\text{-}FeCl_4]^+$ (calculated: m/z = 265.2280). ESI-MS (- ve): m/z = 197.8073 $[FeCl_4]^-$ (calculated: m/z = 197.8074). Elemental Analysis: Obs. C, 44.32; H, 6.99; N, 7.09. Calc. C, 41.50; H, 6.31; N, 6.05. ICP-OES (% weight): Obs. Fe, 11.54. Calc. Fe, 12.06. Characteristic IR bands (cm^{-1}): 3154-3140 (C-H sp^2), 2958-2841 (C-H sp^3), 1684 (C=C/C=N), 1582 (C-C/C-N), 1168(C-O), 1091 (C-O), 838 (C-H sp^2), 735 (C-H sp^2). Raman (cm^{-1}): 335, 332, 142, 112 (Fe-Cl). $[\alpha]_D^{25} =$ +52.2 (c = 5 mg/1 mL MeOH). T_d (10%) = 210 ºC and T_g = 8 ºC. UV-Vis [λmax/nm (ε/$M^{-1}\cdot cm^{-1}$)]: 318 (20167), 364 (16333). μ_{eff} = 6.08 μ_B/molecule. (Fig. S16, S17, S25, S38, S39, S44 and S49).

Catalytic experiments

1.665 mmol of epoxide was mixed with 0.083 mmol of the Fe-based ionic liquid in a glass vial with a magnetic stirrer. Then, the vial was placed in a small reactor with a volume of 2 mL and the reactor was flushed with carbon dioxide (CO_2) three times before the pressure was kept constant (2 bar). After 24 h of reaction at the desired temperature, the reactor was slowly depressurized. The product was purified by extraction with diethyl ether (2×5 mL) and filtration with SiO_2 by flash chromatography. Afterwards, the solvent was evaporated. The residue analyzed by ^{1}H NMR to determine conversion and selectivity and by GC to determine the %*ee*.

RESULTS AND DISCUSSION

The Fe-containing CILs **5**–**9** were prepared in a two-step synthetic strategy (Scheme 1, for further details see sections *Synthesis of chiral imidazolium-based ionic liquids* and *Synthesis of iron-containing ionic liquids*). First, the imidazolium-based CILs **1**–**4** were prepared according to procedures described in the literature.[23,24] Then, 1 equivalent of FeX_3 (X = Cl or Br) was mixed with 1 equivalent of the corresponding imidazolium-based

CILs **1**–**4** in a Schlenk flask under Ar atmosphere. After stirring for 12 h at 90 ºC, the Fe-based CILs **5**–**9** were obtained (Scheme 1).

The synthesized CILs **1**–**4** were characterized by polarimetry, ESI-MS, TGA, ATR FT-IR spectroscopy, and ^{1}H and ^{13}C NMR spectroscopy. In addition, the structures of **1** and **4** were confirmed by X-ray diffraction analysis (for further details see section *Synthesis of chiral imidazolium-based ionic liquids*) and are depicted in Fig. 2 and Fig. S51-52 (Supporting Information). On the other hand, due to the paramagnetic nature of Fe-containing ILs, NMR is not an appropriate spectroscopic tool to analyze ACMILs. Instead, the Fe-containing ionic liquids **5**–**9** were fully characterized by the use of a wide range of techniques, including polarimetry, TGA, DSC, ICP-OES, EA, ESI- Mass, magnetic susceptibility measurements, and UV-vis, ATR FT-IR and Raman spectroscopies.

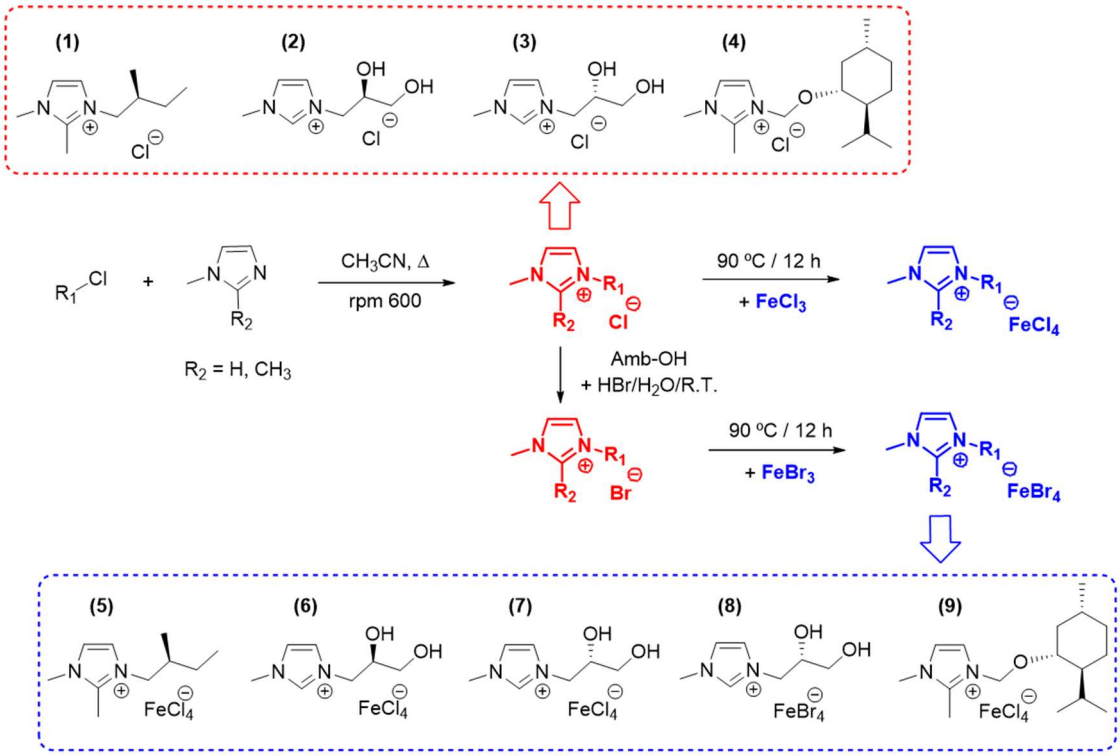

Scheme 1. Chemical structures and acronyms of CILs and ACMILs prepared within a scheme of the synthesis procedure of ACMILs.

All of the ACMILs exhibit specific rotation, which proves the chirality of these compounds (Table 1). The sodium D line (589 nm) was used as incident light since ILs and ACMILs do not absorb light at this frequency. All ACMILs prepared, excepting **9**, show similar optical activity than their respective chiral precursors. From data in table 1, it seems reasonable to propose that specific rotation values ($[\alpha]_D^{25}$) of iron-based CILs are

influenced by the size of the chiral building block. The more sterically hindered the IL, the higher the $[\alpha]_D^{25}$ absolute value. Consequently, both $[\alpha]_D^{25}$ and size of the chiral moiety follow the trend **9** > **8**/**7**/**6** > **5.** The specific rotation dependence on solvent and temperature has also been studied for **9** (See Supporting Information, Table S1 and Fig. S50). **9** showed different $[\alpha]_D^{25}$ in protic and aprotic solvents with diverse polarities. In addition, the specific rotation of **9** increase at higher temperatures.

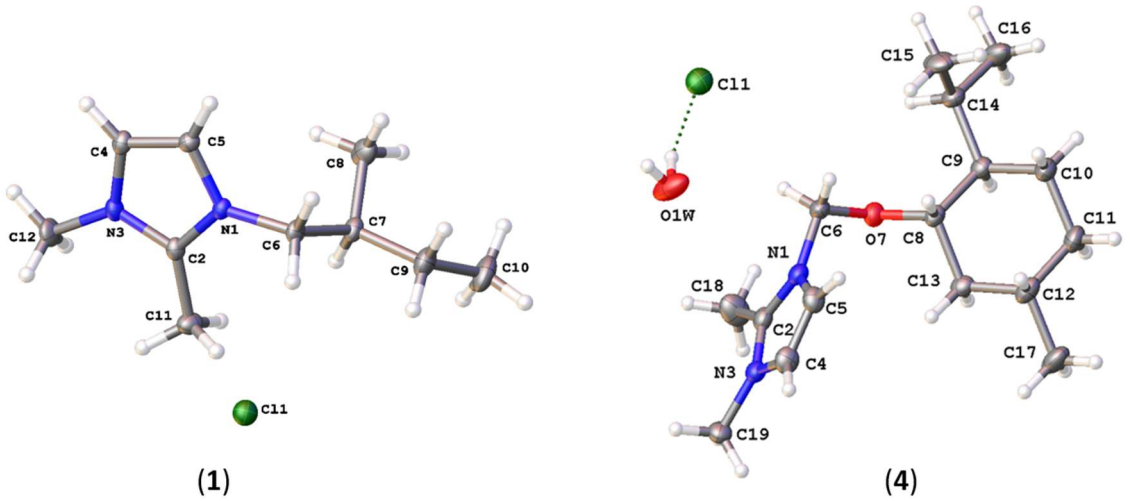

(**1**) (**4**)

Fig. 2 X-ray molecular structures for CILs **1** and **4**. C = grey, Cl = green, H = white, N = blue, O = red. Selected bond lengths (Å) and angles (º) for **1**: N(1)–C(2)=1.339(3); N(1)–C(5)=1.387(3); N(1)–C(6)=1.476(3); C(2)–N(3)=1.339(3); C(2)–C(11)=1.483(3); N(3)–C(4)=1.383(3); N(3)–C(12)=1.469(3); C(4)–C(5)=1.351(3); C(2)–N(1)–C(5)=109.37(19), C(2)–N(1)–C(6)=125.54(18); C(5)–N(1)–C(6)=125.08(18); N(1)–C(2)–C(11)=126.1(2); N(3)–C(2)–N(1)=107.34(18); N(3)–C(2)–C(11)=126.6(2); C(2)–N(3)–C(4)=109.42(19); C(2)–N(3)–C(12)=125.51(18); C(4)–N(3)–C(12)=125.07(19); C(5)–C(4)–N(3)=107.08(19); C(4)–C(5)–N(1)=106.79(19); N(1)–C(6)–C(7)=112.19(19); and selected data for **4**: N(1)–C(2)=1.337(4); N(1)–C(5)=1.386(4); N(1)–C(6)=1.478(4); C(2)–N(3)=1.334(4); C(2)–C(18)=1.479(5); N(3)–C(4)=1.383(5); N(3)–C(19)=1.470(4); C(4)–C(5)=1.341(5); C(6)–O(7)=1.388(4); O(7)–C(8)=1.448(3); C(2)–N(1)–C(5)=108.9(3), C(2)–N(1)–C(6)=126.1(3); C(5)–N(1)–C(6)=124.9(3); N(1)–C(2)–C(18)=126.1(3); N(3)–C(2)–N(1)=107.8(3); N(3)–C(2)–C(18)=126.1(3); C(2)–N(3)–C(4)=109.0(3); C(2)–N(3)–C(19)=126.5(3); C(4)–N(3)–C(19)=124.5(3); C(5)–C(4)–N(3)=107.4(3); C(4)–C(5)–N(1)=106.9(3); O7(2)–C(6)–N(1)=112.1(2); C(6)–O(7)–C(8)=115.3(2); O(7)–C(8)–C(9)=108.8.

Table 1 Specific rotations of the so-obtained CILs and Fe-containing ILs.[a]

Entry	Chiral IL	$[\alpha]_D^{25}$	ACMIL	$[\alpha]_D^{25}$
1	**1**	-2.4	**5**	-2.6
2	**2**	+15.6	**6**	+12.2
3	**3**	-16.0	**7**	-13.6
			8	-18.4
4	**4**	+112.0	**9**	+52.2

[a] c = 5 mg/mL, MeOH, 25 ºC.

Table 2 summarizes the most important physical properties of **5**–**9**. The thermal stability of ACMILs was studied by TGA (Table 2 and Fig. 3a). All curves display two marked zones corresponding to different weight loss ranges. The first region is associated with the imidazolium cation decomposition. The second mass loss at higher temperature is related to the decomposition of the metal complex anion. The thermal decomposition temperature (T_d) of ILs at 10% weight loss are 334, 259, 257, 275 and 210 ºC for **5**, **6**, **7**, **8** and **9**, respectively. All compounds are stable up to 200 ºC and, excepting **5**, show lower T_d than their respective CILs precursors (See Supporting Information, Fig. S26-S29). Interestingly, the T_d of ACMILs is strongly dependent on the structure of the imidazolium cation (size and composition). The relative stability order of ACMILs is **5** > **6**/**7**/**8** > **9**. This trend correlates with the chiral moiety size of ILs (2-methylbutyl < 2.3-dihydroxypropyl < menthoxymethyl), since the smaller the size, the higher the thermal stability. (for further details see Supporting Information, Fig. S30, S32, S34, S36 and S38).

Table 2 Physical properties of synthesized chiral Fe-containing ILs **5**–**9**.

ACMIL	Physical State[a]	Yield (%)	$[\alpha]_D^{25}$[b]	T_g (ºC)[c]	T_d (ºC)[d]
5	Dark green liquid	99	-2.6	-63	334
6	Dark green liquid	99	+12.2	-35	259
7	Dark green liquid	99	-13.6	-34	257
8	Orange liquid	99	-18.4	-31	275
9	Green sticky solid	99	+52.2	8	210

[a] Physical State at 20 ºC. [b] $[\alpha]_D^{25}$: c = 5 mg/mL, MeOH, 25 ºC. [c] Glass transition temperature (T_g) determined by DSC.[d] Thermal decomposition temperature (T_d) determined by TGA at 10% weight loss of the IL analyte.

DSC was employed to study the phase transition of ACMILs (Table 2 and Fig. 3b). All

ACMILs are liquid at R.T., excepting **9** whose physical state is semi-solid. The glass transition temperature (T_g) values for **5**, **6**, **7**, **8** and **9** are -69, -35, -34, -31 and 8 ºC, respectively (see Supporting Information, Fig. S31, S33, S35, S37 and S39). Once again, the thermal property T_g is strongly dependent on the imidazolium size.[25]

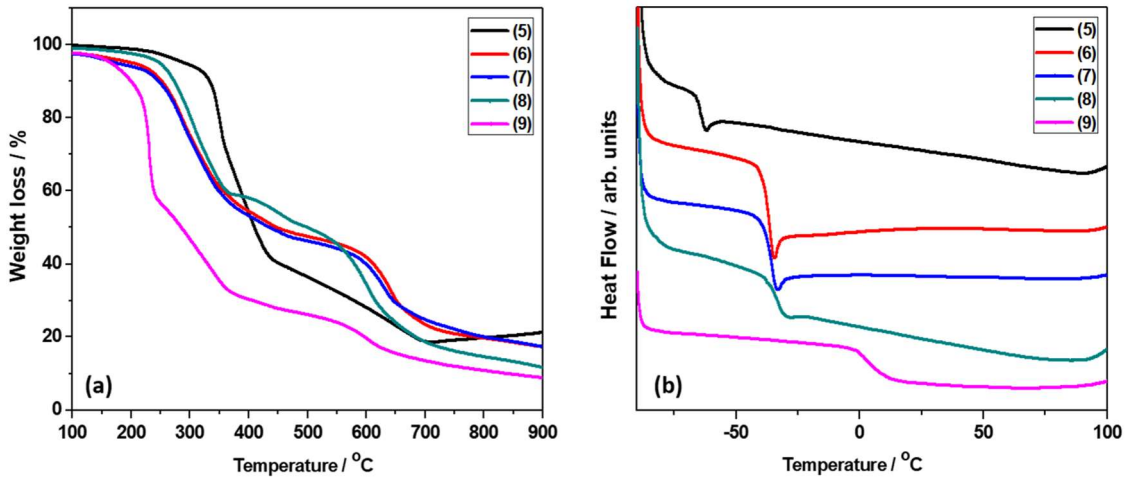

Fig. 3 (a) TGA curve of **5-9** from 100 to 900 ºC. (b) DSC curves of **5-9** from -90 to 100 ºC upon heating (second cycle; heating rate: 10 ºC/min).

5–**9** were further analysed by ATR FT-IR and Raman spectroscopies. All FT-IR spectra of ACMILs (Fig. 4a) show weak bands at about 3100 cm^{-1} associated with C-H bonds of the aromatic imidazolium ring. These spectra also display discernible vibrations in the region *ca.* 2960-2840 cm^{-1}, which are allocated to H-C-H asymmetric stretching vibrations of aliphatic groups attached to the imidazolium ring.[26] In this zone, other weak bands are assigned to vibrations corresponding to the C-H on the aromatic ring. In addition, peaks detected around 3180-3080 cm^{-1} indicate the presence of OH groups for **6, 7** and **8**.[27] Finally, intense bands are observed at low frequencies range (from 400 to 1700 cm^{-1}). Bands around 1690-1170 cm^{-1} correspond to C=N and C-N stretch.[28] For **9**, the asymmetric C-O-C stretching mode also appears in this region, specifically at 1166 cm^{-1}.[29]

Raman data can give a clue about the metal coordination environment of the complex anion (Table 3 and Fig. 4b). The Raman-active modes observed belong to the tetrahedral symmetry group of the $[FeX_4]^-$ iron complex (X = Cl and Br), specifically to the stretching modes of the Fe–X bond. These data agree with the values reported in the literature for other compounds containing the same halometallate ions.[30]

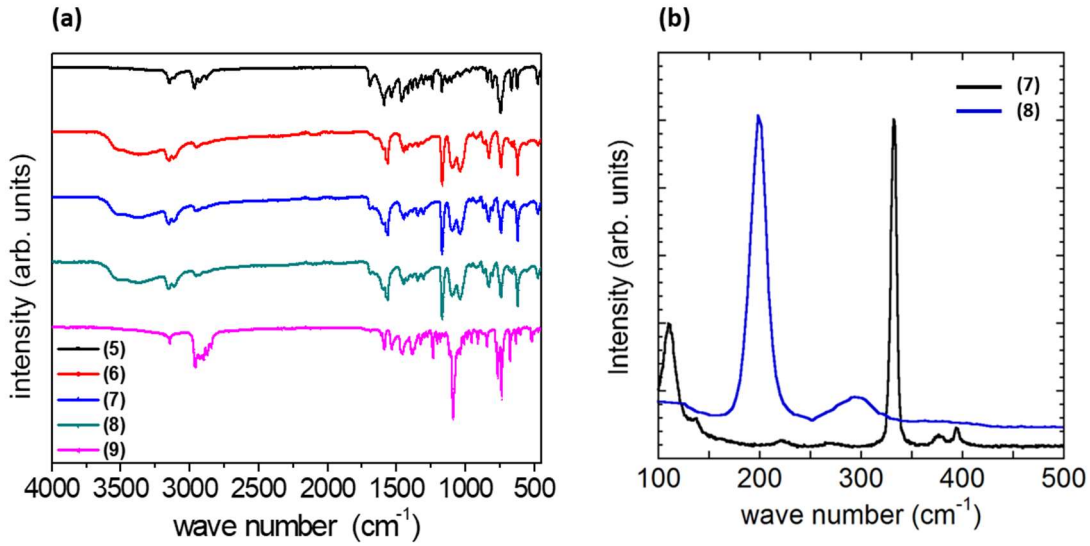

Fig. 4 (a) Comparative FT-IR spectra of **5**–**9**. (b) Comparative non-polarized Raman spectra of two representative samples (**7** and **8)** in the range 100–500 cm^{-1}.

Table 3 Vibrational assignment (cm^{-1}) for the Raman spectra (from 100 to 400) of **5**-**9** at R.T.

Compound Assignment	Raman Frequency (cm^{-1})				
	5	**6**	**7**	**8**	**9**
Fe–X (X = Cl or Br) sym bend	110	108	111	-	112
Fe–X (X = Cl or Br) asym bend	141	138	140	-	142
Fe–X (X = Cl or Br) sym stretch	332	328	330	198	332
Fe–X (X = Cl or Br) asym stretch	334	330	332	284	335

UV-vis absorption spectra of ACMILs **5**-**7** and **9** are very similar, with two peaks around 316 and 364 nm which are typical for charge-transfer absorptions of $[FeCl_4]^-$ (Fig. 5).[31,32] On the other hand, **8** displays a different absorption spectrum with three peaks at 394, 426 and 473 nm, assigned to ligand to metal charge transfer bands of $[FeBr_4]^-$ anion (Fig. 5).[31,32] Consequently, all the ACMILs synthetized exhibit absorption spectra that confirm the presence of the $[FeX_4]^-$ anion.

DC magnetic susceptibility measurements were carried out for the ACMILs. These analyses were performed in the temperature range 2−300 K. The dependence of reciprocal molar magnetic susceptibilities (χ_m^{-1} and $\chi_m T$) on temperature is presented in Fig. S45-49 (Supporting Information). Calculated values for the effective paramagnetic moments (μ_{eff}) and the paramagnetic Curie temperatures (θ) are gathered in Table 4. μ_{eff} displays values between 5.88 and 6.09 (μ_B/molecule), which are in good accord with the expected one of 5.92 μ_B for d^5 Fe(III) ions with high-spin S = 5/2 state.[33] $\chi_m T$ do not shows

any clear trend in the range from 4.27 to 4.67 emuK/molOe at R.T. (Table 4), but agrees well with the predicted value of 4.375 emuK/molOe for Fe^{3+} ion.[30,34] In addition, only **9** exhibits a magnetization M at 50 kOe similar to the expected fully saturated value of 5 μ_B/Fe for a Fe^{3+} ion. The other ACMILs display lower M than the theoretical saturation magnetization moment, but are in a good agreement with those previously reported for FeX_4-based ILs (X = Cl or Br).[30] Magnetism measurements at different temperatures are provided in the supporting Information (see Fig. S45-S49).

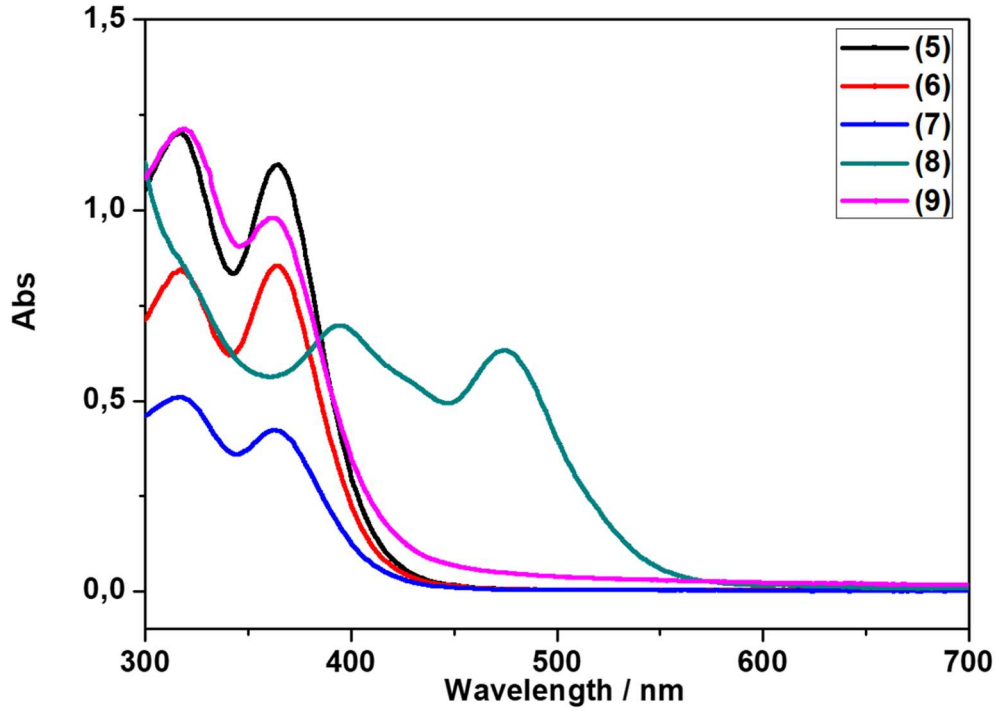

Fig. 5 Comparative UV-vis spectra of **5**–**9**.

Table 4 Magnetic Data for (**5**–**9**).[a]

ACMIL	μ_{eff} (μ_B/molecule)	$\chi_m T$ (emuK/molOe)	θ (K)	M (μ_B/molecule)
5	5.88 (1)	4.56 (1)	-1.75 (1)	3.30 (1)
6	5.89 (1)	4.27 (1)	-2.80 (1)	3.82 (1)
7	5.88 (1)	4.29 (1)	-3.63 (1)	3.78 (1)
8	6.09 (1)	4.67 (1)	-16.0 (1)	2.00 (1)
9	6.08 (1)	4.40 (1)	-0.44 (1)	4.91 (1)

[a] Paramagnetic effective moments (μ_{eff}) per molecule extracted from the Curie-Weiss fitting of the magnetic susceptibility ($\chi_m T$), paramagnetic Curie temperature (θ) and value of the magnetization (M) at 50 kOe and 2 K.

Finally, we performed the kinetic resolution of a racemic mixture of styrene oxide through the asymmetric cycloaddition of CO_2 to epoxides catalyzed by Fe-containing chiral ionic liquids **5** and **9** (Table 5). Although the enantiomeric excesses observed are very low, this preliminary experiment serves as a proof of concept for the potential application of ACMILs as enantioselective catalysts.

Table 5. Kinetic resolution of racemic mixture of styrene oxide by cycloaddition of CO_2 catalyzed by Fe-based chiral ionic liquids **2** and **3**.[a]

Entry	Catalyst	T (ºC)	Time (h)	Conv. (%)[b]	Selectivity (%)[c]	%*ee* (epoxide)[d]
1	**5**	R.T.	24	58	85 : 12 : 3	4
2	**9**	0	7	21	77 : 18 : 5	6

[a] Reagents and conditions: 5 mol % of ACMILs, styrene oxide (1.665 mmol), 24 h, neat and p(CO_2) = 2.0 bar. [b] Conversions determined by ^{1}H NMR spectroscopy and refer to the selective conversion of styrene oxide (average of two runs).[c] % selectivity referred to **A** : **B** : **C**. [d] %*ee* were determined by GC (average of two runs).

CONCLUSIONS

We present the synthesis and characterization of four based on different imidazolium cations. These compounds were used as enantioselective precursors to prepare five acidic chiral paramagnetic ionic liquids through an easy synthetic method. The obtained ACMILs were fully characterized using polarimetry, ICP-OES, EA, and UV-vis, ATR FT-IR and Raman spectroscopies. In addition, the magnetic properties of these chiral iron-based ionic liquids were studied, showing a Fe^{3+} oxidation state with a magnetic spin S = 5/2. UV-vis measurements corroborate the presence of the $[FeX_4]^-$ anion in all the ACMILs, while Raman studies confirm a tetrahedral symmetry for this species. We have also performed the thermal characterization of these novel ACMILs by TGA and DSC, which display liquid physical state and high thermal stability (up to 200 ºC). These new ACMILs combine simultaneously the optical, magnetic and acidic properties of $[FeX_4]^-$ anions with the chiral features of imidazolium cations. Such interesting properties envisage a new approach to develop ACMILs with applications in enantioselective catalysis (e.g. CO_2 fixation into cyclic carbonates) or chiral recognition agents, among others.

AUTHOR INFORMATION

Corresponding Authors

*E-mail: mmgandul@us.es (Carmen Martín).

*E-mail: israel.canorico@nottingham.ac.uk (Israel Cano)

ORCID

Carmen Martín: 0000-0001-8687-6887

Israel Cano: 0000-0003-3727-9327

CONFLICTS OF INTEREST

There are no conflicts of interest to declare.

ACKNOWLEDGMENTS

Financial support from the Spanish Ministerio de Ciencia e Innovación (Projects MAT2014-55049-C2-R and MAT2016-75883-C2-1-P) and Universidad del País Vasco/Euskal Herriko Unibertsitatea (GIU17/50 and PPG17/37). Carmen Martín is grateful to the Proyecto Puente convocatoria 2018 from Universidad de Cantabria financed by SODERCAN and VI PPIT-2018 from Universidad de Sevilla. Israel Cano acknowledges financial support from the European Community through a Marie Skłodowska-Curie Individual Fellowships (IF-EF; Programme/Call: H2020-MSCA-IF-2015; Proposal No: 704710–Sdchirnanocat).

NOTES AND REFERENCES

1 K. Dong, X. Liu, H. Dong, X. Zhang, S. Zhang, Multiscale studies on ionic liquids, *Chem. Rev.*, 2017, **117**, 6636-6695, DOI: 10.1021/acs.chemrev.6b00776.

2 P. Wasserscheid, T. Welton, *Ionic liquids in synthesis*, John Wiley & Sons, 2008, DOI: 10.1002/9783527621194.

3 M. Galinski, A. Lewandowski, I. Stepniak, Ionic liquids as electrolytes, *Electrochim. Acta*, 2006, **51**, 5567-5580, DOI:10.1016/j.electacta.2006.03.016.

4 P. Hapiot, C. Lagrost, Electrochemical reactivity in room-temperature ionic liquids, *Chem. Rev.*, 2008, **108**, 2238- 2264, DOI: 10.1021/cr0680686.

5 A. S. Amarasekara, Acidic ionic liquids. *Chem. Rev.*, 2016, 116, 6133-6183, DOI: 10.1021/acs.chemrev.5b00763.

6 C. Chiappe, S. Rajamani, Structural effects on the physico-chemical and catalytic properties of acidic ionic liquids: an overview, *Eur. J. Org. Chem.*, 2011, **2011**, 5517-5539, DOI: 10.1002/ejoc.201100432.

7 J. Estager, J. Holbrey, M. Swadźba-Kwaśny, Halometallate ionic liquids–revisited*, Chem. Soc. Rev.*, 2014, **43**, 847-886, DOI: 10.1039/C3CS60310E.

8 Y. Katayama, I. Konishiike, T. Miura, T. Kishi, Redox reaction in 1-ethyl-3-methylimidazolium–iron chlorides molten salt system for battery application, *J. Power Sources*, 2002, **109**, 327-332, DOI: 10.1016/S0378-7753(02)00077-0.

9 M. Valkenberg, W. Hölderich, Friedel-Crafts acylation of aromatics catalysed by supported ionic liquids, *Appl. Catal. A: General*, 2001, **215**, 185-190, DOI: 10.1016/S0926-860X(01)00531-2.

10 M. Vasiloiu, P. Gaertner, K. Bica, Iron catalyzed Michael addition: Chloroferrate ionic liquids as efficient catalysts under microwave conditions, *Sc. China Chem*., 2012, **55***,* 1614-1619, DOI: 10.1007/s11426-012-4657-z.

11 H. Wang, R. Yan, Z. Li, X. Zhang, S. Zhang, Fe-containing magnetic ionic liquid as an effective catalyst for the glycolysis of poly(ethylene terephthalate), *Catal. Comm*., 2010, 11, 763-767, DOI: 10.1016/j.catcom.2010.02.011.

12 R. Kore, P. Berton, S. P. Kelley, P. Aduri, S. S. Katti, R. D. Rogers, Group IIIA halometallate ionic liquids: Speciation and applications in catalysis, *ACS Catal*., 2017, **7**, 7014-7028, DOI: 10.1021/acscatal.7b01793.

13 M. Li, S. L. De Rooy, D. K. Bwambok, B. El-Zahab, J. F. DiTusab, I. M. Warner, Magnetic chiral ionic liquids derived from amino acids, *Chem. Commun*., 2009, 6922-6924, DOI: 10.1039/b917683g.

14 L. W. Qian, X. L. Hu, P. Guan, X. Q. Guo, Bi-Functional magnetical chiral ionic liquids derived from imidazolium and pyridinium, *Appl. Mech. Mater*., 2012, 128-133, DOI: 10.4028/www.scientific.net/AMM.161.128.

15 P. González-Izquierdo, O. Fabelo, G. Beobide, O. Vallcorba, F. Sce, J. Rodríguez Fernández, M.T. Fernández-Díaz, I. de Pedro, Magnetic structure, single-crystal to single-crystal transition, and thermal expansion study of the (Edimim)[$FeCl_4$] halometalate compound, *Inorg. Chem.*, 2018, **574**, 1787-1795, DOI: 10.1021/acs.inorgchem.7b02632.

16 F. Scé, I. Cano, C. Martin, G. Beobide, Ó. Castillo, I. de Pedro, Comparing conventional and microwave-assisted heating in PET degradation mediated by imidazolium-based halometallate complexes, *New J. Chem*., 2019, 43, 3476-3485, DOI: 10.1039/C8NJ06090H.

17 S. Cot, M. K. Leu, A. Kalamiotis, G. Dimitrakis, V. Sans, I. de Pedro, I. Cano, An oxalate-bridged binuclear iron(III) ionic liquid for the highly efficient glycolysis of polyethylene terephthalate (PET) under microwave irradiation, *ChemPlusChem*, 2019, **84**, 786-793, DOI : 10.1002/cplu.201900075.

18 M. K. Leu, I. Vicente, J. A. Fernandes, I. de Pedro, J. Dupont, V. Sans, P. Licence, A. Gual, I. Cano, On the real catalytically active species for CO_2 fixation into cyclic carbonates under near ambient conditions: Dissociation equilibrium of [BMIm][$Fe(NO)_2Cl_2$] dependant on reaction temperature*, App. Catal. B Environ*., 2019, **245**, 240-250, DOI: 10.1016/j.apcatb.2018.12.062.

19 W. L. F. Armarego, D. D. Perrin, *Purification of Laboratory Chemicals*, Butterworth-Heineman, Oxford (UK), 1997.

20 O. V. Dolomanov, L. J. Bourhis, R. J. Gildea, J. A. K. Howard, H. Puschmann, *J. Appl. Cryst*. 2009, **42**, 339-341, DOI: 10.1107/S0021889808042726.

21 L. J. Bourhis, O. V. Dolomanov, R. J. Gildea, J. A. K. Howard, H. Puschmann, *Acta Cryst*., 2015, **A71**, 59-75, DOI: 10.1107/S2053273314022207.

22 G. M. Sheldrick, *Acta Cryst*., 2015, **C71**, 3-8, DOI: 10.1107/S2053229614024218.

23 Racemic [diOHPrMIm]Cl: F. Bellina, A. Bertoli, B. Melai, F. Scalesse, F. Signori, C. Chiappe, Synthesis and properties of glyceryl imidazolium based ionic liquids: a promising class of task-specific ionic liquids, *Green Chem.*, 2009, **11**, 622-629, DOI: 10.1039/B821927C.

[R-diOHPrMIm]Cl: G. Fukuhara, C. Chiappe, A. Mele, B. Melai, F. Bellina, Y. Inoue, Photochirogenesis in chiral ionic liquid: enantiodifferentiating [4+4] photocyclodimerization of 2-anthracenecarboxylic acid in (R)-1-methyl-3-(2,3-dihydroxypropyl)imidazolium bistriflimide, *Chem. Commun.*, 2010, **46**, 3472-3474, DOI: 10.1039/c002448a.

[S-diOHPrMIm]Cl: H. Gao, L. Shi, S. Zhang, J. Li, X. Wang, L. Zheng, Aggregation behavior of imidazolium-based chiral surfactant in aqueous solution, *Colloid Polym. Sci.*, 2013, **291**, 1077-1084, DOI: 10.1007/s00396-012-2830-8.

24 S. Mumtaz, I. Cano, N. Mumtaz, A. Abbas, J. Dupont, H. Yasmeen Gondal, Supramolecular interaction of non-racemic benzimidazolium based ion pairs with chiral substrates, *Phys. Chem. Chem. Phys.*, 2018, **20**, 20821-20826, DOI: 10.1039/c8cp03881c.

25 J. D. Holbrey, K. R. Seddon, The phase behaviour of 1-alkyl-3-methylimidazolium tetrafluoroborates; ionic liquids and ionic liquid crystals, *J. Chem. Soc. Dalton Trans*., 1999, 2133-2140, DOI: 10.1039/A902818H.

26 E. R. Talaty, S. Raja, V. J. Storhaug, A. Dölle, W. R. Carper, Raman and infrared spectra and ab initio calculations of $C_{2\text{-}4}$MIM imidazolium hexafluorophosphate ionic liquids, *J. Phys. Chem. B*, 2004, **108**, 13177-13184, DOI: 10.1021/jp040199s.

27 Y. Q. Cai, Y. Liu, G. H. Gao, Synthesis and application of an IL-supported diol as protecting group for aldehydes, *Chin. Chem. Lett.*, 2007, **18**, 1205-1208, DOI: 10.1016/j.cclet.2007.07. 012.

28 N. E. Heimer, R.E. Del Sesto, Z. Meng, J.S. Wilkes, W. R. Carper, Vibrational spectra of imidazolium tetrafluoroborate ionic liquids, *J. Mol. Liq.*, 2006, **124**, 84-95, DOI: 10.1016/j.molliq. 2005.08.004.

29 Z. Fei, W. H. Ang, D. Zhao, R. Scopelliti, E. E. Zvereva, S. A. Katsyuba, P. J. Dyson, Revisiting ether-derivatized imidazolium-based ionic liquids, *J. Phys. Chem. B*, 2007, **111**, 10095-10108, DOI: 10.1021/jp073419l.

30 A. García-Saiz, I. de Pedro, O. Vallcorba, P. Migowski, I. Hernández, L. Fernández-Barquin, I. Abrahams, M. Motevalli, J. Dupont, J.A. Gonzalez, J.R. Fernández, 1-Ethyl-2,3 dimethylimidazolium paramagnetic ionic liquids with 3D magnetic ordering in its solid state: synthesis, structure and magneto-structural correlations, *RSC Adv.*, 2015, **5**, 60835-60848, DOI: 10.1039/C5RA05723J.

31 K. B. Yoon, J. K. Kochi, Ferric iodide as a nonexistent compound, *Inorg. Chem.*, 1990, **29**, 869-874, DOI: 10.1021/ic00329a058.

32 A. Abedi, N. Safari, V. Amani, H. R. Khavasi, Synthesis, characterization, mechanochromism and photochromism of $[Fe(dm_4bt)_3][FeCl_4]_2$ and $[Fe(dm_4bt)_3][FeBr_4]_2$, along with the investigation of steric influence on spin state, *Dalton Trans*., 2011, **40**, 6877-6885, DOI 10.1039/C0DT01508C.

33 Y. Yoshida, G. Saito, Influence of structural variations in 1-alkyl-3-methylimidazolium cation

and tetrahalogenoferrate(III) anion on the physical properties of the paramagnetic ionic liquids, *J. Mater. Chem.*, 2006, **16**, 1254-1262, DOI: 10.1039/b515391c.

34 A. García-Saiz, P. Migowski, O. Vallcorba, J. Junquera, J. A. Blanco, J. A. González, M. T. Fernández-Díaz, J. Rius, J. Dupont, J. Rodríguez-Fernández, I. de Pedro, A magnetic ionic liquid based on tetrachloroferrate exhibits three-dimensional magnetic ordering: A combined experimental and theoretical study of the magnetic interaction mechanism, *Chem. Eur. J*., 2014, **20**, 72-76, DOI: 10.1002/chem.201303602.